

## Research Note

# H $\alpha$ imaging of the local volume galaxies

## I. The NGC 6946 galaxy group

I. D. Karachentsev<sup>1</sup>, S. S. Kajsın<sup>1</sup>, Z. Tsvetanov<sup>2</sup>, and H. Ford<sup>2</sup>

<sup>1</sup> Special Astrophysical Observatory, Russian Academy of Sciences, N.Arkhыз, KChR, 369167, Russia  
e-mail: [ikar@luna.sao.ru](mailto:ikar@luna.sao.ru)

<sup>2</sup> Department of Physics and Astronomy, Johns Hopkins University, Baltimore, MD 21218, USA

Received 11 January 2005 / Accepted 11 February 2005

**Abstract.** We present new H $\alpha$  imaging of all known dwarf irregular companions to NGC 6946: UGC 11583, KK 251, KK 252, KKR 55, KKR 56, Cepheus 1, KKR 59, and KKR 60. The galaxies span a range of blue absolute magnitudes of  $[-13.6, -17.6]$ , relative gas content of  $[0.1, 2.5] M_{\odot}/L_{\odot}$ , current star formation activity of  $[0.2, 5.2] \times 10^{-2} M_{\odot} \text{ yr}^{-1}$ , and timescale to exhaust the current gas supply of  $[6, 86]$  Gyr.

**Key words.** galaxies: dwarf – stars: formation

### 1. Introduction

In a volume-limited sample, dwarf galaxies constitute the vast majority of the total galaxy population. Yet, their star formation histories remain poorly understood. Up until 2003, among the 362 known neighboring galaxies with distances  $D < 8$  Mpc, of which dwarfs constitute about 85% (Karachentsev et al. 2004), only  $\sim 15\%$  have been imaged in the fundamental H $\alpha$  line. Recent observations obtained by Gil de Paz et al. (2003), James et al. (2004), Helmboldt et al. (2004), and Hunter & Elmegreen (2004) significantly advanced our understanding of star formation properties of nearby dwarf galaxies. Nevertheless, the present knowledge of the local star formation rate, determined by a cumulative H $\alpha$  flux of the galaxies in the Local Volume (LV), remains very incomplete. For a substantial improvement of this situation, we started a program to obtain H $\alpha$  images of all 214 northern (Dec  $> 0^{\circ}$ ) dwarf galaxies within 8 Mpc, having angular diameters  $a_{25} < 8'$  compatible with the SAO 6-m telescope CCD camera field of view. We believe that this project will also be supported by systematic H $\alpha$  imaging of all southern neighboring dwarf galaxies. As a result, we anticipate to get the first complete data on the H $\alpha$  luminosity function of galaxies in the Local Universe and the total H $\alpha$  flux of all galaxies within a distance of 8 Mpc.

In addition, we intend to prepare the first Atlas of H $\alpha$  images for a complete sample of the LV galaxies, which can be compared with existing sets of their HI maps. The creation of such a complete reference sample at zero redshift is fundamental for studying the evolution of star formation in

distant galaxy samples (like the Hubble Deep Field), as well as the relation between star formation activity and galaxy environment. We note that many LV galaxies are objects that have been discovered only recently. In particular, about a hundred such galaxies were found on POSS-II plates by Karachentseva and her co-workers over the last few years. Most of the LV galaxies are targets of the ongoing Snapshot Survey with the Wide Field and Planetary Camera 2 and Advanced Camera for Surveys aboard the Hubble Space Telescope (programs 8192, 8601, 9771 and 10235), for which accurate distances are determined using the tip of the red giants branch method. This gives us a unique possibility to compare their H $\alpha$  structure with high resolution images in the  $V, I$  bands and correctly determine their luminosities.

Here, we present the first results from our H $\alpha$  imaging program for all 8 dwarf irregular (dIr) companions to the bright spiral galaxy NGC 6946. In follow up papers, we will study the rate of star formation in other nearest groups, as well as in the general local field.

### 2. Observations and data reduction

We obtained H $\alpha$  and red continuum CCD images for the eight known members of the NGC 6946 group during 3 observing runs between September 2001 and November 2002. A typical seeing was about  $1.7''$ . These observations were carried out at the SAO 6-m telescope using an imaging camera equipped with a  $2048 \times 2048$  pixel CCD. The pixel scale was  $0.25''/\text{pixel}$ . The area imaged was  $6' \times 6'$ . The H $\alpha$  + [NII] emission line fluxes

**Table 1.** Basic properties of the galaxies.

| Object    | $a$  | $b/a$ | $B_t$ | $V_h$              | $V_{LG}$           | $M_B$  | $M_{HI}/L$            | $A(H\alpha)$ | $F_{H\alpha} \times 10^{13}$         | $F_c \times 10^{13}$                 | $SFR$                        | $t_{gas}$ |
|-----------|------|-------|-------|--------------------|--------------------|--------|-----------------------|--------------|--------------------------------------|--------------------------------------|------------------------------|-----------|
| (1)       | (2)  | (3)   | mag   | km s <sup>-1</sup> | km s <sup>-1</sup> | mag    | $M_{\odot}/L_{\odot}$ | mag          | erg s <sup>-1</sup> cm <sup>-2</sup> | erg s <sup>-1</sup> cm <sup>-2</sup> | $M_{\odot}$ yr <sup>-1</sup> | Gyr       |
| UGC 11583 | 1.8  | .44   | 15.90 | 127                | 430                | -14.28 | 2.04                  | 0.71         | 0.29 ± .04                           | 0.56                                 | 0.0025                       | 86        |
| KK 251    | 1.6  | .50   | 16.5  | 130                | 433                | -13.63 | 2.41                  | 0.69         | 0.31 ± .20                           | 0.58                                 | 0.0026                       | 54        |
| KK 252    | 0.9  | .99   | 16.7  | 138                | 441                | -14.11 | 0.10                  | 1.05         | 0.16 ± .03                           | 0.42                                 | 0.0018                       | 8.4       |
| NGC 6946  | 11.5 | .85   | 9.58  | 51                 | 355                | -20.86 | 0.21                  | 0.80         | 339                                  | 708                                  | 3.12                         | 3.1       |
| KKR 55    | 0.6  | .67   | 17.0  | 32                 | 337                | -14.79 | 0.34                  | 1.58         | 0.48 ± .04                           | 2.06                                 | 0.0091                       | 6.3       |
| KKR 56    | 0.7  | .64   | 17.6  | -47                | 260                | -14.39 | 0.52                  | 1.69         | 0.10 ± .09                           | 0.47                                 | 0.0021                       | 29        |
| Ceph 1    | 3.0  | .50   | 15.4  | 58                 | 367                | -17.53 | 0.70                  | 2.18         | 0.66 ± .18                           | 4.92                                 | 0.0216                       | 67        |
| KKR 59    | 2.3  | .61   | 15.7  | 1                  | 311                | -17.01 | 0.30                  | 2.08         | 1.75 ± .23                           | 11.9                                 | 0.0523                       | 7.4       |
| KKR 60    | 0.7  | .70   | 18.   | -35                | 275                | -15.42 | -                     | 2.46         | 0.84 ± .27                           | 8.10                                 | 0.0356                       | -         |

were obtained by observing each galaxy through two filters: a narrow-band ( $\sim 70$  Å) interference filter centered on  $6567$  Å, and a broad  $R$ -band filter (SED707,  $\lambda_{cen} = 6780$  Å,  $\Delta\lambda = 1100$  Å) to determine the nearby continuum level. Integration times were typically  $2 \times 300$  s in the  $R$  band and  $2 \times 600$  s in  $H\alpha$ . Because of a small range of radial velocities, we use the same  $H\alpha$  filter for all objects.

The data reduction was performed using standard MIDAS package tasks. The following steps were taken to obtain continuum-free  $H\alpha + [NII]$  images. First, the images were bias subtracted and flat fielded by a median twilight sky flat taken through the appropriate filter. After automatic cosmic rays removal, the sky subtraction was done by fitting a surface underneath the object of interest using the areas away from the object. Because the seeing was slightly different in different images, we match the seeing by degrading all the images to the worst one.

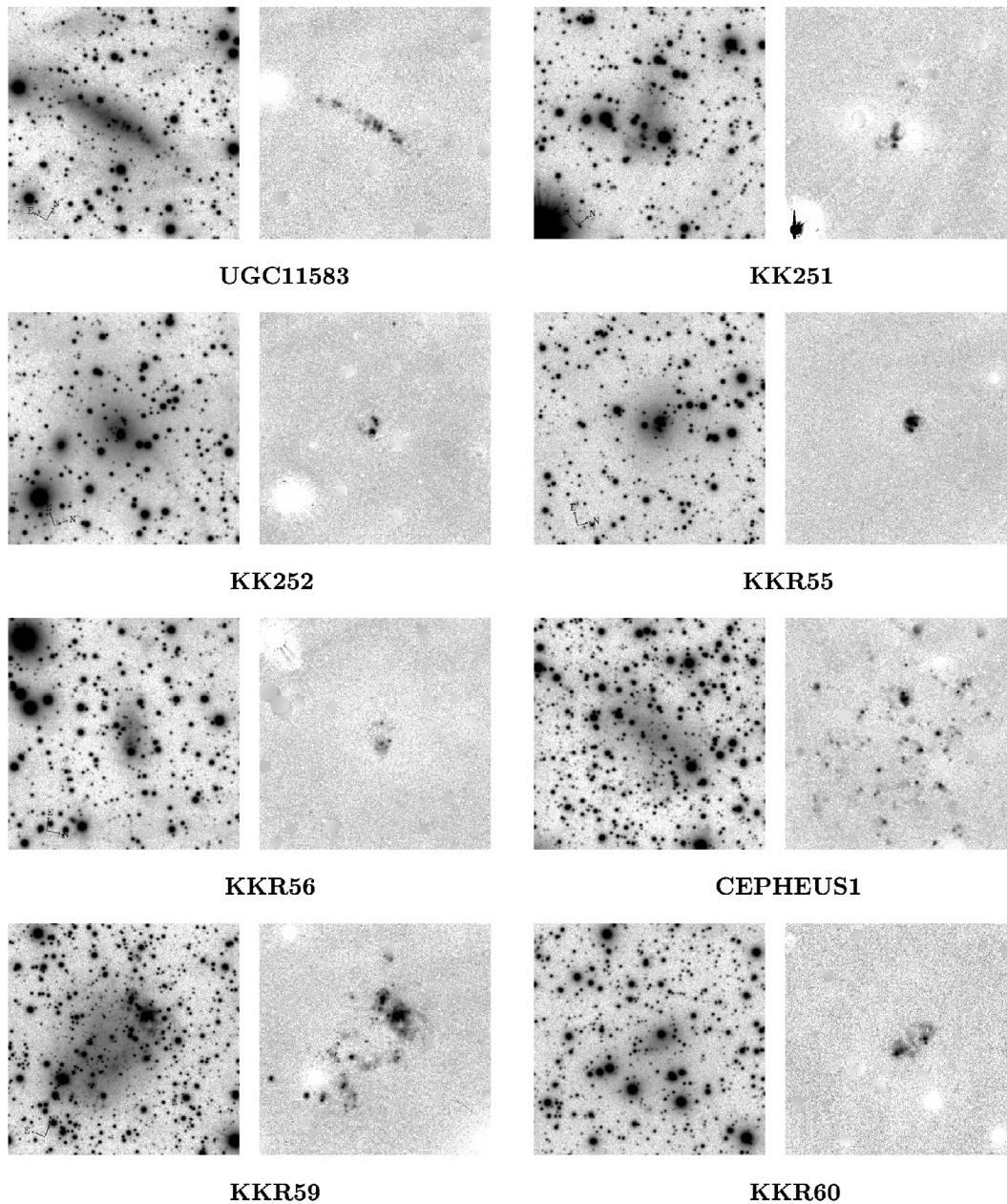
Finally, to obtain  $H\alpha + [NII]$  continuum-free images, the  $R$ -band images were scaled relative to the interference filter images using 10–15 unsaturated stars, and then subtracted from the interference filter images. Flux calibration for the images was made with the observations of Oke (1990) standard stars. The typical errors in total  $H\alpha$  fluxes due to background sky subtraction and photometric calibration are within 10% (apart from the KK 251 observed during a non-photometric night).

Figure 1 presents (from left to right) the  $H\alpha$  on-line, and the continuum-free images of the eight observed galaxies. Residuals in the continuum-subtracted images due to the presence of very bright saturated field stars were removed interactively.

### 3. Results

The basic parameters of nine galaxies in the NGC 6946 group are listed in Table 1. Column 1 contains the number of each galaxy in the Uppsala Galaxy Catalogue (UGC) or in the lists by Karachentseva & Karachentsev (1998, KK) and Karachentseva et al. (1999, KKR); Cols. 2, 3 gives major angular diameter in arcminutes and apparent axial ratio measured at a level of  $\sim 25^m/\square''$ ; Col. 4 presents the integrated apparent  $B$ -magnitude; Cols. 5, 6 give the heliocentric radial velocity derived by Makarov et al. (2003) or Huchtmeier et al. (2000a,b, 2003), and the radial velocity with respect to the Local Group centroid under the apex parameters according to Karachentsev & Makarov (1996); Col. 7 presents the absolute magnitude corrected for the Galactic extinction,  $A_B$ , according to Schlegel et al. (1998); Col. 8 lists the hydrogen mass-to-blue luminosity ratio from Karachentsev et al. (2004); Col. 9 presents the Galactic extinction  $A(H\alpha) = 0.538A_B$ ; Cols. 10, 11 give the observed total  $H\alpha + [NII]$  flux with its standard error and the total flux corrected for the Galactic extinction; Col. 12 lists the star formation rate,  $SFR(M_{\odot} \text{ yr}^{-1}) = 1.27 \times 10^9 F(H\alpha)D^2$ , where  $D$  is the galaxy distance in Mpc, and  $F(H\alpha)$  is in units of  $\text{erg s}^{-1} \text{ cm}^{-2}$ ; and the last column gives the time (in Gyr) to exhaust the total current gas content of the galaxy at the current star formation rate,  $(\text{Total Gas Mass})/(SFR)$ , where the total gas mass is  $1.32 \times M(HI)$  to account for He. For the bright spiral NGC 6946 its  $H\alpha$  flux in Col. 10 was taken from Young et al. (1996), corresponding to the inner 6 arcmin region only.

Almost all the group galaxies have been resolved into stars by Sharina et al. (1997) and Karachentsev et al. (2000), who



**Fig. 1.** From left to right: the  $H\alpha$ , and the continuum-free images of eight observed galaxies around NGC 6946. **UGC 11583.** The large-scale image of this elongated irregular galaxy (Karachentsev et al. 2000) reveals several stellar associations in its body. The continuum-subtracted  $H\alpha$  image (top right in Fig. 1) shows a dozen of compact HII-regions aligned along the major axis. We did not find any appreciable diffuse  $H\alpha$  emission in UGC 11583 with an upper limit of about  $0.05 \times 10^{-13} \text{ erg s}^{-1} \text{ cm}^{-2}$ . **KK 251.** This dIrr galaxy is situated only  $6'$  away from UGC 11583. Its continuum-subtracted  $H\alpha$  image shows three compact HII-knots and several diffuse emission regions on the galaxy southern side. **KK 252.** The well-resolved face-on dIrr galaxy (Karachentsev et al. 2000). Four very compact HII-regions are seen in its central part as well as faint diffuse emission at the southern side. **KKR 55.** It may be considered as a blue compact dwarf (BCD) galaxy with a relatively bright stellar association at  $8''$  NE off the center. The continuum-subtracted  $H\alpha$  image of KKR 55 finds a strong knotted HII-region, which coincides with the association. No appreciable diffuse emission is seen in the remaining parts of the galaxy. **KKR 56.** The well-resolved dIrr galaxy (Karachentsev et al. 2000). The continuum-subtracted  $H\alpha$  image shows several almost stellar-like faint knots embedded into a faint diffuse envelope. **Cepheus 1.** This Sm-type very obscured galaxy has been discovered in HI by Burton et al. (1999), who estimated the galaxy distance as 6.0 Mpc based on the luminosity of its HII regions. The continuum-subtracted  $H\alpha$  image obtained by us confirms the presence of many isolated compact and diffuse HII regions scattered over the area much exceeding the visible galaxy body. Probably, the central South-to-North elongated part of Cepheus1 seen in continuum is only a brighter bar-like structure of a low surface brightness disk outlined by HII regions. **KKR 59.** The resolved irregular galaxy has two large “curly” HII regions on its northern edge. Several other diffuse emission knots are seen over the galaxy body. This is the most  $H\alpha$  luminous dwarf companion to NGC 6946. **KKR 60.** Unlike other galaxies considered here, KKR 60 is not resolved into stars so far. The continuum-subtracted  $H\alpha$  image shows several compact HII regions within a diffuse emission component. The heliocentric  $H\alpha$  radial velocity of KKR 60,  $-35 \text{ km s}^{-1}$ , is typical one for the group members.

determined the mean distance to the group via the brightest stars to be  $(5.9 \pm 0.4)$  Mpc. This value was used by us to calculate the galaxy absolute magnitudes and SFRs given in table.

#### 4. Discussion

Until the 1990s, the giant spiral NGC 6946 was considered as an isolated galaxy situated on the edge of the Local Void (Tully 1988). Recent discoveries of eight companions establish NGC 6946 as the brightest member of a loose group. The root mean relative velocity of companions is  $(-2 \pm 24)$  km s<sup>-1</sup>, showing no asymmetry with respect to NGC 6946. The mean square radial velocity dispersion of the companions, 64 km s<sup>-1</sup>, and the mean projected linear separations, 245 kpc, are typical for a loose group dominated by a late type galaxy. The virial mass-to-blue luminosity ratio for the NGC 6946 group,  $30 M_{\odot}/L_{\odot}$ , is also characteristic for the nearby groups.

Ferguson et al. (1998) presented deep  $H\alpha$  image of NGC 6946, which reveal the presence of HII regions out to two standard optical radii,  $R_{25}$ . Young et al. (1996) determined the total  $H\alpha$  flux from the inner (6') region of the galaxy. Comparing the data on Col. 11, we find that 96% of the total  $H\alpha$  flux of the NGC 6946 group comes from its brightest spiral galaxy. This result is consistent with the conclusion of Nakamura et al. (2003) based on the Sloan Digital Sky Survey that 83% of the blue luminosity density comes from spiral galaxies, 5% from irregular galaxies and 9% from early type ones. Therefore, in the present epoch, the disks of massive spiral galaxies are the basic hearths of current star formation activity.

The distribution of the NGC 6946 companions in integrated star formation rate spans a range from 0.002 to 0.052 in  $M_{\odot} \text{ yr}^{-1}$  that is typical for irregular galaxies (see Fig. 5 in Hunter & Elmegreen 2004). The median timescale to exhaust the current gas supply for the dIr companions to NGC 6946,  $t_{\text{gas}} = 29$  Gyr, is one order longer than the timescale for the NGC 6946 itself. The gas depletion timescale  $t_{\text{gas}}$  for the group members is also typical for the sample of dIr galaxies in (Hunter & Elmegreen 2004).

*Acknowledgements.* This research was supported by RFFI–DFG grant 02–02–04012 and RFFI grant 04–02–16115.

#### References

- Burton, W. B., Braun, R., Walterbos, R. A., & Hoopes, C. G. 1999, *AJ*, 117, 194
- Ferguson, A., Wyse, R., Gallagher, J., & Hunter, D. 1998, *ApJ*, 506, L19
- Gil de Paz, A., Madore, B. F., & Pevunova, O. 2003, *ApJS*, 147, 29
- Helmboldt, J. F., Walterbos, R. A., Bothun, G. D., et al. 2004, *ApJ*, 613, 914
- Huchtmeier, W. K., Karachentsev, I. D., Karachentseva, V. E., & Ehle, M. 2000a, *A&AS*, 141, 469
- Huchtmeier, W. K., Karachentsev, I. D., & Karachentseva, V. E. 2000b, *A&AS*, 147, 187
- Huchtmeier, W. K., Karachentsev, I. D., & Karachentseva, V. E. 2003, *A&A*, 401, 483
- Hunter, D. A., & Elmegreen, B. G. 2004, *AJ*, 128, 2170
- James, P. A., Shane, N. S., Beckman, J. E., et al. 2004, *A&A*, 414, 23
- Karachentsev, I. D., & Makarov, D. I. 1996, *AJ*, 111, 794
- Karachentseva, V. E., & Karachentsev, I. D. 1998, *A&AS*, 127, 409
- Karachentseva, V. E., Karachentsev, I. D., & Richter, G. M. 1999, *A&AS*, 135, 221
- Karachentsev, I. D., Sharina, M. E., & Huchtmeier, W. K. 2000, *A&A*, 362, 544
- Makarov, D. I., Karachentsev, I. D., & Burenkov, A. N. 2003, *A&A*, 405, 951
- Karachentsev, I. D., Karachentseva, V. E., Huchtmeier, W. K., & Makarov, D. I. 2004, *AJ*, 127, 2031
- Miller, B. W., & Hodge, P. 1994, *ApJ*, 427, 656
- Nakamura, O., Fukugita, M., Yasuda, N., et al. 2003, *AJ*, 125, 1682
- Oke, J. B. 1990, *AJ*, 99, 1621
- Schlegel, D. J., Finkbeiner, D. P., & Davis, M. 1998, *ApJ*, 500, 525
- Sharina, M. E., Karachentsev, I. D., & Tikhonov, N. A. 1997, *Astron. Lett.*, 23, 373
- Tully, R. B. 1988, *Nearby Galaxy Catalogue* (Cambridge: Cambridge Univ. Press)
- Young, J. S., Allen, L., Kenney, J. D., Lesser, A., & Rownd, B. 1996, *AJ*, 112, 1903
- van Zee, L. 2000, *AJ*, 119, 2757